MACH NUMBER DISTRIBUTION OVER THE AXIS OF SUPERSONIC UNDEREXPANDED JETS

Yu. P. Finat'ev, L. A. Shcherbakov, and N. M. Gorskaya

UDC 532.522

The limiting flow parameters are determined directly behind the central shock for Mach numbers M ≫ 1 in front of the shock. A formula for the Mach number distribution over the jet axis is derived.

Interest in underexpanded supersonic jets has increased during the past years owing to their increased utilization in a variety of technological fields. Lack of exact analytical methods, which would permit complete determination of the structure of an underexpanded jet, as well as the extensive computational labor involved in the method of characteristics and the incompleteness of results obtained by it, have made it necessary to develop experimental studies. The authors of the present paper have studied gas jets expelled into a gas-filled space for the following range of parameters:

$$M_a = 1 - 4.85;\ P_a/P_\infty = 10 - 10^4;\ \varkappa = 1.3 - 1.67;$$
$$T_0 = 289 - 700\ ^\circ\mathrm{K};\ \alpha = 8 - 21^\circ.$$

The experiments were performed in a low-pressure wind tunnel in a pulsed mode of operation. This made it necessary to employ a quick-response measuring and parameter-recording system. Pressure was measured with induction and resistance pressure gauges, and temperature with a thermocouple; sensor signals were recorded with a loop oscillograph. The test data were used to derive a relation for the distance to the central shock [6]

$$\frac{x_0}{d_a} = 3{,}2\ \frac{M_a^2}{M_a^2 + 1}\ n^{0.39}. \qquad (1)$$

The experiments revealed the following.

1. No dependence of the distance to the central shock is observed on $\varkappa$ (within the range from 1.3 to 1.67), on the aperture half-angle of the nozzle α (for α = 8 to 21°), nor on the gas temperature T_0 (for T_0 = 289 to 700°K).

2. The ratio of the active to passive pressure $n = P_a/P_\infty$ and the Mach number M_a are the principal parameters which define the position of the central shock.

3. The increase in the ratio x_0/d_a with increasing P_a/P_∞ is less pronounced than indicated by the data in [1, 9].

4. At $M_a > 3.5$, the ratio P_a/P_∞ becomes the principal parameter defining the position of the central shock.

The solution of some actual problems requires knowledge of the parameters behind the central shock. At large ratios P_a/P_∞, when M ≫ 1 in front of the central shock, the problem of determining the parameters behind the central shock can be simplified. Assuming that the flow along the jet axis from the nozzle exit section to the central shock is one-dimensional and isentropic and that relations derived for a direct

Institute of Chemical Physics, Academy of Sciences of the USSR, Moscow. Translated from Inzhenerno-Fizicheskii Zhurnal, Vol. 15, No. 6, pp. 982-987, December, 1968. Original article submitted March 5, 1968.

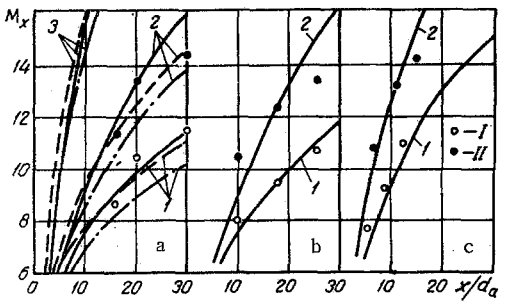

Fig. 1

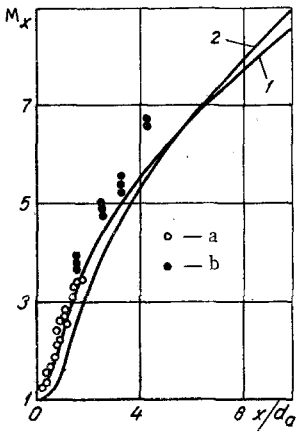

Fig. 2

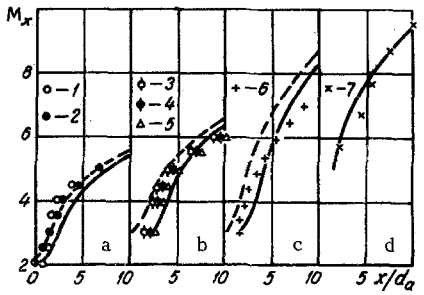

Fig. 3

Fig. 1. Comparison of computations from formula (10) (solid curves) with the experiment (points): a) $M_a = 1$ [– – –) calculation by a method used in [1]; – · – · –) method of characteristics]; 1) I refers to $\varkappa = 1.3$; 2) II refers to $\varkappa = 1.4$; 3) refers to $\varkappa = 1.67$; b) $M_a = 2$; 1) I refers to $\varkappa = 1.3$; 2) II refers to $\varkappa = 1.4$; c) 1) I refers to $\varkappa = 1.3$; $M_a = 3.1$ and 3.12; 2) II refers to $\varkappa = 1.4$; $M_a = 3.0$ and 2.8.

Fig. 2. Comparison of computations from formula (10) for $M_a = 1$; $\varkappa = 1.4$ with Owen and Thornhill's data [3, 7] and with the experiment: 1) Owen and Thornhill; a) n = 3.92 to 4.5; $P_a \leq 5$ techn. atm; 2) formula (10); b) n = 200 to 1000; $P_a \sim 50$ techn. atm.

Fig. 3. Comparison of computations from formulas (10) and (11) (solid curves) and from formula (10) (dashed curves) with computations by the method of characteristics [2, 4]: a) $M_a = 2$; $\varkappa = 1.15$; data [2]: 1) n = 56.5; $\alpha = 0°$; 2) n = 56.5; $\alpha = 15°$; b) $M_a = 3$; $\varkappa = 1.15$; data [2]: 3) n = 6080; $\alpha = 0$; 4) n = 62.9; $\alpha = 0$; 5) $M_\infty = 5$; $\alpha = 0$; c) $M_a = 3.1$; $\varkappa = 1.25$; data [2]: 6) n = 62.9; $\alpha = 0$; d) $M_a = 4.2$; $\varkappa = 1.2$; data [4]: 7) $n = \infty$; $\alpha = 8.3°$.

shock are valid for the central shock,† it can be proved that the value of M_1 becomes almost constant starting from M = 5-6 to ∞.

M_1 can be expressed through M with the aid of the relation

$$M_1 = \sqrt{\frac{2 + (\varkappa - 1) M^2}{2\varkappa M^2 - (\varkappa - 1)}} = \sqrt{\frac{\frac{2}{M^2} + (\varkappa - 1)}{2\varkappa - \frac{\varkappa - 1}{M^2}}}. \tag{2}$$

When $M \to \infty$, we obtain at the limit

$$\lim_{M \to \infty} M_1 = \sqrt{\frac{\varkappa - 1}{2\varkappa}}. \tag{3}$$

In the same manner we obtain other limiting parameter relations

$$\lim_{M \to \infty} \frac{P_{01}}{P_1} \left[\frac{(\varkappa + 1)^2}{4\varkappa}\right]^{\frac{\varkappa}{\varkappa - 1}}, \tag{4}$$

$$\lim_{M \to \infty} \frac{\rho_{01}}{\rho_1} = \left[\frac{(\varkappa + 1)^2}{4\varkappa}\right]^{\frac{1}{\varkappa - 1}}, \tag{5}$$

$$\lim_{M \to \infty} \frac{T_{01}}{T_1} = \frac{(\varkappa + 1)^2}{4\varkappa}, \tag{6}$$

$$\lim_{M \to \infty} q_1 = \frac{\rho_1 w_1}{\rho_1^* a^*} = \left(\frac{2\varkappa}{\varkappa + 1}\right)^{\frac{1}{2} \frac{\varkappa + 1}{\varkappa - 1}} \left(\frac{\varkappa - 1}{2\varkappa}\right)^{\frac{1}{2}}. \tag{7}$$

†Strictly speaking, the central shock is a direct shock only at the point of intersection with the jet axis, and is close to a direct shock at other points; the flow is subsonic at all points directly behind the shock.

TABLE 1. Limiting Flow Parameters behind the Central Shock for Some Values of $\varkappa$

$\varkappa$	M_1	$\frac{P_{01}}{P_1}$	$\frac{\rho_{01}}{\rho_1}$	$\frac{T_{01}}{T_1}$	$q=\frac{\rho_1 w_1}{\rho_1^* a^*}$
1,15	0,255	1,04	1,034	1,005	0,4
1,2	0,2886	1,061	1,051	1,010	0,465
1,3	0,3391	1,075	1,058	1,017	0,541
1,4	0,3782	1,109	1,076	1,030	0,604
1,67	0,4478	1,189	1,105	1,069	0,699

Table 1 shows numerical values of the limiting relations for some values of $\varkappa = c_p/c_v$. The experiments showed that starting with n = 6-7, the Mach number M in front of the central shock is greater than 4. Thus, the limiting relations are fulfilled within a high accuracy for n values ranging from 10 to ∞.

The stagnation temperature of the gas does not change in the passage through the shock, $T_{01} = T_0$. Consequently, if T_0 is known, T_1 can be readily determined with the aid of the limiting relation. In order to determine the other parameters, the pressure behind the central shock must be known.

In [3], it is suggested that the static pressure P_1 behind the central shock is equal to the ambient pressure P_∞. We have checked this hypothesis experimentally. For small ratios P_a/P_∞ at $\varkappa = 1.4$, it proved possible to conduct the experiment under steady-state conditions. The influence of time lag was thus eliminated, and P_1 and P_{01} were measured with a Prandtl tube and a Pitot tube, respectively. The measurement data are compiled in Table 2, from which it can be seen that for ratios $P_a/P_\infty = 3$ to 5, the static pressure behind the central shock exceeds the ambient pressure, in spite of the ratio P_{01}/P_1 being close to its limiting value.

For ratios $P_a/P_\infty > 30$, only pulsed operation was possible, where a large error arises in the measurement of static pressure P_1 behind the shock, owing to the time lag of the manometric system (composed of a Prandtl tube and induction gauge) because of the small orifice cross sections at the lateral surface of the Prandtl tube. The situation is further aggravated by the inability of a Prandtl tube to measure pressures directly behind the shock. Because of this, we measured the pressure P_{01} from which P_1 can be computed with the aid of the limiting parameter relations. The measurements obtained for $\varkappa = 1.3$ and 1.4 are compiled in Table 2. All measurements refer to the jet axis.

The data compiled in Table 2 reveal only a slight discrepancy between the pressures P_1 and P_∞ for a rather large range of P_a/P_∞ ratios. This verifies the hypothesis proposed in [3]. Assuming that the flow* is one-dimensional and adiathermal, we write the energy equation for regions directly in front and behind the central shock, in the form

$$\frac{1}{2} w^2 + \frac{\varkappa}{\varkappa - 1} \frac{P}{\rho} = \frac{1}{2} w_1^2 + \frac{\varkappa}{\varkappa - 1} \frac{P_1}{\rho_1}. \tag{8}$$

By assuming that $\rho_1/\rho = (\varkappa + 1)/(\varkappa - 1)$ for $M \to \infty$ and $P_1 = P_\infty$, with the aid of elementary transformations we arrive at the expression

$$\frac{P_a}{P_\infty} = n = \frac{\varkappa^2 - 1}{4\varkappa} \frac{\left(1 + \frac{\varkappa - 1}{2} M^2\right)^{\frac{1}{\varkappa - 1}}}{\left(1 + \frac{\varkappa - 1}{2} M_a^2\right)^{\frac{\varkappa}{\varkappa - 1}}}. \tag{9}$$

Expression (9) relates the Mach number M at the jet axis in front of the central shock to the pressure ratio $n = P_a/P_\infty$. By assuming that the Mach number distribution over the jet axis up to the central shock is independent of n [2, 3] and using the empirical relation (1), we obtain an expression for the Mach number distribution over the jet axis

$$\frac{x}{d_a} = 3.2 \left(\frac{\varkappa^2 - 1}{4\varkappa}\right)^{0.39} \frac{1}{1 + 1/M_a^2} \frac{\left(1 + \frac{\varkappa - 1}{2} M^2\right)^{\frac{0.39}{\varkappa - 1}}}{\left(1 + \frac{\varkappa - 1}{2} M_a^2\right)^{\frac{0.39\varkappa}{\varkappa - 1}}}. \tag{10}$$

*The flow behind the central shock is assumed to be isentropic.

TABLE 2. Measurement Results for Pressures P_1 and P_{01} behind the Central Shock

$\varkappa$	M_a	P_∞, mm Hg	P_0, abs. atm	$n=\frac{P_a}{P_\infty}$	P_{01}, mm Hg	P_1, mm Hg	P_1/P_∞
		750	7,33	3,92	1250	1010	1,35
		741	7,8	4,5	1180	975	1,31
	1,0	757	7,85	4,37	1215	837	1,11
		140	89,0	255,0	150,0	135,0	0,963
		274	86,5	127,0	304	274	1,0
		22	25,0	455,0	22	19,8	0,9
	1,55	755	7,67	1,95	1290	1220	1,62
1,4		40	38,5	91,5	44	39,6	0,99
	2,0	8	18,0	22,0	8	7,2	0,9
		60	43,0	69,5	60	54,0	0,9
		60	40,5	18,9	67	60,2	1,005
	2,8	40	37,5	26,2	44	39,6	0,99
		60	48,5	22,6	83	74,6	1,24
		6	6,5	450,0	6	5,4	0,9
	1,0	104	35,0	140,0	100	90,0	0,865
		70	46,0	273,0	92	83,0	1,185
1,3		42	45,0	112,0	62	55,8	1,33
	1,97	154	47,0	32,0	176	158,0	1,025
		158	46,0	30,5	195	175,5	1,11
		76	49,0	9,8	70	63,0	0,83
	3,125	60	49,0	12,4	66	59,5	0,99

Relation (10) was experimentally checked for air and carbon dioxide jets at Mach numbers between 1 and 3.4, the pressure P_{01} being measured at three points on the jet axis. The Mach number was determined from the ratio P_{01}/P_0 on the basis of the formula for the direct shock or from gasdynamic tables. The results presented in Fig. 1 confirm relation (10).

The influence of low pressure on the Mach number distribution over the jet axis can be judged from Fig. 2. In this figure, the experimental points for the dense ($P_a \sim 50$ techn. atm) and less dense ($P_a \leq 5$ techn. atm) jets coincide essentially with the Owen–Thornhill curve, and are also close to the data computed from formula (10). The large scatter of points for n = 200 to 1000 may be attributed to experimental uncertainty in the pulse mode.

The influence of low-pressure on the results of measurements performed with a Pitot tube could be neglected in our experiments, since the Reynolds number of the flow past the tube was greater than 10^2 [8].

Figure 3 shows a comparison of computations from formula (10) with computations by the method of characteristics [2, 4]. The results agree best for the case where the relative length of the potential flow core for parallel ejection from the nozzle, i.e., the quantity

$$\frac{x_{pot}}{d_a} = \frac{\sqrt{M_a^2 - 1}}{2}. \tag{11}$$

is added to the right-hand side of expression (10).

At large distances from the nozzle exit section, this correction has almost no effect on the shape of the curve, while at small distances it is justified, since formula (10) was obtained under the assumption that $M \gg 1$ in front of the central shock. The solid curves in Fig. 3 were plotted with allowance for correction (11). In this way, formula (10) correlates well with data computed for small values of $\varkappa$ ($\varkappa$ = 1.15 to 1.25) [2, 4].

NOTATION

n	is the ratio of passive to active pressure;
M	is the Mach number;
P	is the gas pressure;
ρ	is the gas density;
T	is the absolute gas temperature;
$\varkappa = c_p/c_v$	is the ratio of specific heats;
α	is the half-apex angle of the nozzle;

x_0 is the distance from the nozzle exit section to the central shock;
w is the gas velocity;
d_a is the diameter of nozzle exit section;
Re is the Reynolds number.

Subscripts

1 denotes behind the direct shock;
a denotes the nozzle exit section;
∞ denotes the ambient medium;
0 denotes the isentropic drag;
01 denotes drag behind the direct shock;
* denotes critical.

Subscripts denote the gas parameters.

LITERATURE CITED

1. Krist, Sherman, and Glass, Raket. Tekhn. i Kosm., No. 1 (1966).
2. C. J. Wang and J. B. Peterson, Jet Propulsion, 28, No. 5 (1958).
3. T. C. Adamson and J. A. Nicholls, J. Aerospace Sci., 26, 16-24 (1959).
4. Pesik, Koppang, and Simkin, Voprosy Raketnoi Tekhniki, No. 12 (1966).
5. L. Howarth (editor), Current Status of High-Speed Aerodynamics [Russian translation], Vol. 1, IL (1955).
6. Yu. P. Finat'ev, L. A. Shcherbakov, and N. M. Gorskaya, Proceedings of the All-Union Conference on Heat and Mass Transfer, Minsk, Vol. 1, Heat and Mass Transfer in the Interaction between Bodies and Gas and Liquid Flows [in Russian], Izd-vo Énergiya, Moscow (1968).
7. J. Scott and J. Dewrie, in: Characteristics of Aerodynamic Molecular Beams: Interaction between Gases and Surfaces [Russian translation], Moscow (1965).
8. Daum, Sheng, and Elliot, Raket. Tekhn. i Kosm., No. 8 (1965).
9. Louis and Carlson, Raket. Tekhn. i Kosm., No. 4 (1964).